FACTA UNIVERSITATIS
Series: **Electronics and Energetics** Vol. 29, No 4, December 2016, pp. 509 - 541
DOI: 10.2298/FUEE1604509P

P-CHANNEL MOSFET AS A SENSOR AND DOSIMETER OF IONIZING RADIATION

Milić M. Pejović

University of Niš, Faculty of Elecronic Engineering, Niš, Serbia

Abstract. *This paper presents a study of MOSFETs as a sensor and dosimeter of ionizing radiation. The electrical signal used as a dosimetric parameter is the threshold voltage. The functionality of these components is based on radiation-induced ionization in SiO_2, which results in increase of positive charge trapped in the SiO_2 and interface traps at Si-SiO_2, leads to change in threshold voltage. The first part of the paper deals with analysis of defect precursors created by ionizing radiation, responsible for creation of fixed and switching traps, as well as most important techniques for their separation. Afterwards, the results for sensitive p-channel MOSFETs (RADFETs) are presented, following with results for commercially available MOSFETs applications as a sensors of ionizing radiation.*

Key words: *Fixed traps, fading, MOSFET, RADFET, switching traps, threshold voltage shift*

1. INTRODUCTION

The attention of today's research on the impact of ionizing radiation on MOSFETs is directed in two ways. The first one is the production on MOSFETs with the highest possible resistance to ionizing radiation (radiation hardness), while the other is toward to ionizing radiation dosimeters production. The first report on the use p-channel MOSFET as integrating radiation dosimeter was published in 1970 [1] and this idea was verified by results published in 1974 [2]. Further investigations lead to the manufacture of radiation sensitive p-channel MOSFETs, also known as RAdiation sensitive Field Effect Transistor (RADFET) or pMOS dosimeter [3]. RADFET has been shown to be suitable for dose measurements in various applications, such as diagnostic radiology and radiotherapy [4]-[8], space radiation monitoring [9]-[12], irradiation of food plants [13] and in personal dosimetry [14], [15].

The RADFET radiation-sensitive region, the oxide film layer under the Al-gate is typically 1μm × 200μm × 200μm, i.e., the sensing volume is much smaller than competing integral dose measuring devices as the ionizing chamber or thermoluminescent dosimeter, implying that it can also be used in vivo dosimetry [16], [17]. This property of the RADFET

Received March 22, 2016
Corresponding author: Milić M. Pejović
Universiy of Niš, Faculy of Electronic Engineering, Aleksandra Medvedeva 14, 18000 Niš, Serbia
(e-mail: milic.pejovic@elfak.ni.ac.rs)

also makes it attractive for measurement in the gradient radiation field where the gradient mostly depends on a single space coordinate, like resolving dose of X-ray microbeams or depth dose distribution [18]. The advantages of RADFETs include immediate, non-destructive dosimetric information readout, real time or delayed reading, possible integration with other sensors and/or electronics, wide dose range, accuracy and competitive price [19], [20]. The application of RADFETs for dosimetry is hadron therapy, which is one of the promising radiation modalities in radiotherapy, another field where it is possible to explore their advantages. Hadron therapy includes, fast neutron therapy, proton therapy, heavy ion therapy and boron-neutron capture therapy. It is shown [21] that RADFETs are less sensitive to neutron radiation than the photon or charge particles. On the other hand, a disadvantage of RADFETs is the need for separate calibration in the fields of different modalities and energy. Moreover, RADFETs have a certain range of the total accumulated dose, which depends on the dosimeter type and sensitivity. Once the upper limit of linearity is achieved, the RADFETs need to be replaced. However, recent studies have shown that such RADFETs can be recovered for reuse by storing at room or elevated temperature for a sufficient time [22], [23] or by annealing with current [24], [25].

The dosimetry of ionizing radiation using radiation sensitive MOSFETs is based on converting the threshold voltage shift ΔV_T into radiation dose D. This shift originates in the radiation-induced electron-hole pairs in the gate oxide layer of the transistor which lead to increase in the density of interface traps and build-up or neutralization of positive trapped charge. The sensitivity of RADFETs can be adjusted, which makes them suitable for various applications. For example, sensitivity can be tuned using different gate oxide layer thickness [26], [27], or in some cases by stacking transistors [14], [15]. The sensitivity can also be tuned by applying positive bias on the gate during irradiation [28], [29].

2. THE DEFECTS PRECURSORS CREATED BY IONIZING RADIATION

Ionizing radiation leads to formation of large number of defects in SiO_2 and at SiO_2 - Si interface, which are responsible for MOSFETs threshold voltage shift. The defects which make significant impact to devices performance will be discussed further.

2.1. Photon induced ionization

During gamma or X-ray irradiation photons interact with the electrons in the SiO_2 molecules releasing secondary electrons and holes, i.e., photons break $Si_o - O$ and $Si_o - Si_o$ covalent bonds in the oxide [30] (the index $_o$ is used to denote silicon atom in the oxide). The released electrons (so called "secondary electrons") which are highly energetic, may be recombined by holes at the place of production, or may escape recombination. The secondary electrons that escape recombination with holes travel some distance until they leave the oxide, losing their kinetic energy through the collisions with the bonded electrons in the $Si_o - O$ and $Si_o - Si_o$ covalent bonds in the oxide, releasing more secondary electrons (the latter bond represents an oxygen vacancy).

Each secondary electron, before it has left the oxide or been recombined by the hole, can break a lot of covalent bonds in the oxide producing a lot of new secondary highly energetic electrons, since its energy is usually much higher than an impact ionizing process energy (energy of 18 eV is necessary for the creation of one electron-hole pair [30], i.e., for the molecule ionization). It is obvious that the secondary electrons play a more important role in bond breaking than highly energetic photons, as a consequence of the difference in their effective masses, i.e., in their effective cross sections. The electrons leaving the production place escape the oxide very fast (for several picoseconds), but the holes remain in the oxide.

The holes released in the oxide bulk are usually only temporary, but not permanently trapped at the place of production, since there are no energetically deeper centers in the oxide bulk. The holes move toward one of the interface (SiO_2-Si or SiO_2-gate), depending on the oxide electric field direction, where they have been trapped at energetically deeper trap hole centers [31], [32]. Moreover, even in the zero gate voltage case, the electrical potential due to a work function difference between gate and substrate is high enough for partial or complete moving towards an interface.

2.2. The defects created by secondary electrons in impact ionization

A secondary electrons passing through oxide bulk, break covalent bonds in the oxide by the impact ionization and create $\equiv Si_o - O^{\bullet +} Si_o \equiv$ complex, where $\equiv$ denotes the three $Si_o - O$ bonds ($O_3 \equiv Si_o - O$) and $^\bullet$ denotes the unpaired electron. The formed $\equiv Si_o - O^{\bullet +} Si_o \equiv$ complex is energetically very shallow, representing the temporary hole centre (the trapped holes can easily leave it [33]).

The strained silicon-oxygen bond $\equiv Si_o - O - Si_o \equiv$ mainly distributed near the interfaces can also be easily broken by the passing secondary electrons, usually created non-bridging-oxygen (NBO) centre, $\equiv Si_o - O^\bullet$, and positively charged E' center, $\equiv Si_o^+$ [34] known as a E'_S center [35]. A NBO centre is an amphoteric defect that could be more easily negatively charged than positively by trapping an electron. The NBO as an energetically deeper centre is the main precursor of the traps (defects) in the oxide bulk and the interface regions.

A secondary electron passing through the oxide can also collide with an electron in the strained oxygen vacancy bond $\equiv Si_o - Si_o \equiv$, which is a precursor of a E'_γ centre ($\equiv Si_o^\bullet$) [36], breaking this bond and knocking out an electron. The oxygen vacancy bonds are mainly distributed in the vicinity of the interfa**c**es.

The trapped charge can be positive (oxide trapped holes) and negative (oxide trapped electrons) and the former is more important, since the hole trapping centers more numerous including E'_S, E'_γ and NBO centers, compared with one electron trap centre (NBO). The holes and electrons trapped near the $Si - SiO_2$ interface have the biggest effect on MOSFET characteristics, since they have the strongest influence on the channel carriers.

2.3. Defects created in SiO_2 by hole transport

The holes trapped at $\equiv Si_o^+$ centers formed from oxygen vacancies and strained silicon-oxygen bonds are energetically deep and steady, at which the holes can remain for longer time period, i.e. they can be hardly filled by electrons than some shallowly trapped holes. These centers exist near both interfaces, especially near the $Si - SiO_2$ interface. The

holes created and trapped at the bulk defects, representing energetically shallow centers, are forced to move towards one of the interfaces under the electric field, where they are trapped at deeper traps, since there a lot of oxygen vacancies, as well as a lot of strained silicon-oxygen bonds near the interfaces, grouping all positive trapped charge there. The holes leave the energetically shallow centers in the oxide spontaneously and transporting to the interface (Fig. 1(a)) by hopping process using either shallow centers in the oxide (Fig. 1(b)); the holes "hop" from one to another center or centers in the oxide valence band (Fig. 1(c)) [31], [37]. Fig. 1 displays the hole transport in the space for the positive gate bias (a) and the energetic diagram for the possible mechanisms of this space process (b) and (c).

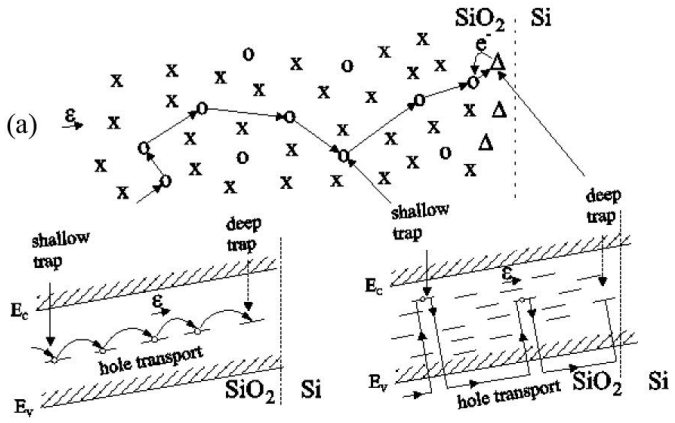

Fig. 1 Space diagram: (a) hole transport through the gate oxide layer in the case of positive gate bias. "x" represents unbroken bonds and "o" broken bonds (trapped holes at shallow traps), respectively, and " Δ " represents the hole trap precursors near the interface (precursors of a deep trap). Energetic diagram: the hole transport (b) by tunneling between to localized traps and (c) by the oxide valence band.

Fig. 2 shows the possible hole (electron) tunneling between adjacent centers: a shallow centre and deep centre. When there is no gate bias (Fig. 2 (a)) the holes (electrons) tunneling between these centers, is not possible. When the transistor is positively biased (Fig. 2 (b)), the bonded electron can tunnel from the deep centre to the shallow centre. It represents the hole tunneling from shallow to deep centers, being permanently trapped at the deep center. The electron, which is now in the shallow centre, can easily tunnel from this shallow centre to the next adjusted shallow centre, enabling the hole transport towards the interface [31].

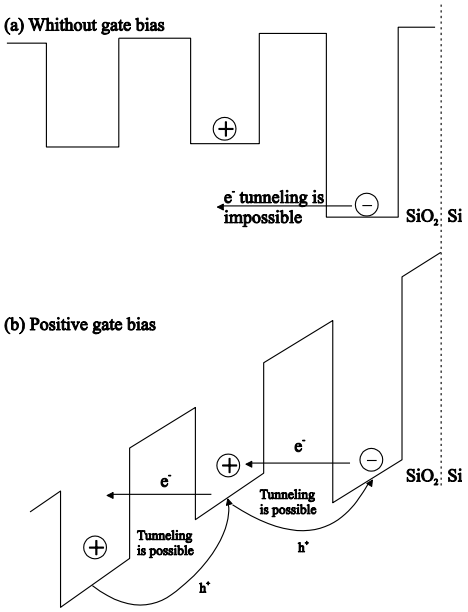

Fig. 2 The electron tunneling between adjacent centers: (a) shallow centre and (b) deep centre.

Moving throughout the oxide, the holes react with the hydrogen defect $\equiv Si_o - H$ and $\equiv Si_o - OH$ finally create E'_S, E'_γ, NBO centers, hydrogen ions H^+ and hydrogen atoms H^o. H^+ ions and H^o atoms were important for defect creation at SiO_2-Si interface (see the next subsection).

When the holes reach the interface, they can break both the strained oxygen vacancy bonds $\equiv Si_o - Si_o \equiv$, forming E'_γ centers [34] and the strained silicon-oxygen bonds $\equiv Si_o - O - Si_o \equiv$, created the E'_S and NBO centers [31]. These centers represent energetically deeper hole and electron trapping centers, respectively. It should be noted that the energetic levels of the defects created after the holes at E'_S, and E'_γ centers and electrons at NBO centre, respectively, have been trapped can be various. The chemically same defects show different behaviors depending on the whole bond structure: the angles and distances between the surrounding atoms [38]-[43].

2.4. Defects created at SiO_2 - Si interface

The defects at the SiO_2-Si interface known as true interface traps represent an amphoteric defect $Si_3 \equiv Si_s^\bullet$ (index $_s$ is used to denote silicon atom in substrate): a silicon atom $\equiv Si_s^\bullet$ at SiO_2-Si interface back bonded to three silicon atoms from the substrate $\equiv Si_s$ usually denoted as $\equiv Si_s^\bullet$ or $Si^\bullet$. They can directly be created by incident photons passing to the substrate or the gate [44], [45] but this amount can be neglected. Interface traps are mainly created by trapped holes (h^+ model) [46]-[49] and by hydrogen released in the oxide (hydrogen-released species model– H model) [50]-[52]. The h^+ model proposes that a hole trapped near the SiO_2-Si interface created interface trap, suggesting that an

electron-hole recombination mechanism is responsible [47]. Namely, when holes are trapped near the interface and electrons are subsequently injected from substrate, recombination occurs. From the energy released by this electron-hole recombination the interface state may be created.

The H model proposes that H^+ ions released in the oxide by trapped holes drift towards SiO_2-Si interact with $\equiv Si_o - H$ and $\equiv Si_o - OH$ defects, drifting toward the SiO_2-Si interface under the positive electric field. When the H^+ ion arrives at the interface, it picks up an electron from the substrate, breaking a highly reactive hydrogen atom H^o [53]. Also, according to the H model the hydrogen atoms H^o released in reaction holes with $\equiv Si_o - H$ and $\equiv Si_o - OH$ defects and diffuse towards the SiO_2-Si interface under the existing concentration gradient. These atoms react without an energy barrier at the interface producing interface trap in interaction with interface trap precursors $\equiv Si_s - H$ and $\equiv Si_s - OH$ [54]-[56]. Interaction between H^o atoms with $\equiv Si_s - H$ and $\equiv Si_s - OH$ precursors, beside creation of interface traps in interaction with interface trap precursors, leads to the creation of H_2 and H_2O molecules, respectively [31], [53]. H_2 molecules diffuse towards the bulk of oxide where it is cracked at CC^+ centers [57]. This cracking process ensured the continuous source of H^+ ions, which drift towards the interface to form interface traps [58].

2.5. Classification of defects according to their influence on I-V characteristics

The above mentioned defects can be divided to fixed traps (FT) and switching traps (ST). FT represents traps in the oxide that do not have an ability to exchange the charge with the channel (substrate) within the transfer/subthreshold characteristic measurement time frame [59]. FT could be either negatively or positively charged, and they attract or repulse the channel carrier by the Coulomb force, depending on the charge sign of both their charge and channel carrier charge. ST represent the traps created near and at SiO_2-Si interface and they do capture (communicate with) the carrier from the channel within the transfer/subthreshold characteristic measurement time frame [59]. The ST created in the oxide near SiO_2-Si interface are called slow switching traps (SST), but the ST created at the interface are called fast switching traps (FST) also called true interface traps. The SST located in the oxide, closed to the SiO_2-Si interface are also known slow states (SS) [60], anomalous positive charge (APC) [61], [62], switching oxide traps (SOT) [63] and border traps [64]. It was emphasized that the influence of FT and ST on the transistor subthreshold characteristics is manifested through the parallel shift and its slope variation, respectively. FT are usually deeper in the oxide, and during the long time post-irradiation annealing they can only be permanently recovered or temporally compensated (as in the case of switching gate bias experiments). It is emphasized that FST are amphoteric, and each of them contributes to two states within the silicon band gap (an acceptor and a donor) which could be randomly distributed inside it.

3. TRANSISTOR CHARACTERIZATION

There are several techniques for FT and ST separation [65]. Most commonly used techniques are subthreshold midgap and charge pumping technique. Their basic principle will be presented.

3.1. Subthreshold midgap technique

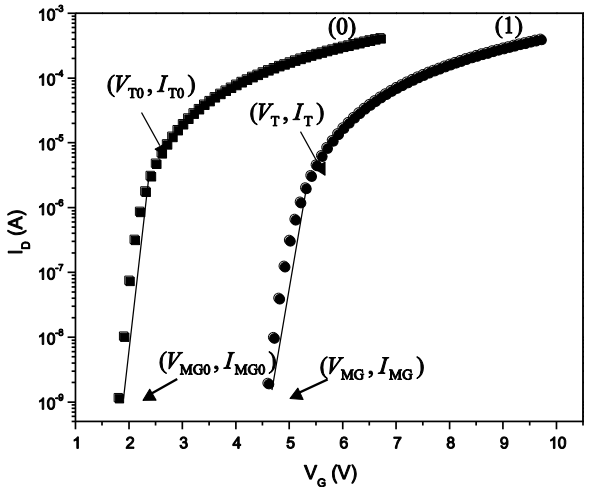

Fig. 3 Subthreshold characteristics of RADFETs with 100 nm thick gate oxide manufactured by Tyndall National Institute, Cork, Ireland: (0) before gamma-ray irradiation and (1) after irradiation to 500 Gy.

The midgap-subthreshold (MG) technique [59] for determination of FT and ST densities is based on analysis of MOSFETs subthreshold characteristics. Namely, the influence of FT and ST on the transistor subthreshold characteristics in saturation is in their parallel shifts and their slope changes, respectively. The first step is linear regression of the linear regions of subthreshold characteristics (Fig. 3). The linear regression gives a straight line $\log(I_D) = m \cdot V_G + n$. The next step in the procedure is the calculation of the midgap current before irradiation, I_{MG0} and after irradiation I_{MG}. The calculation of the midgap current is performed using the subthreshold-current equation for a transistor in saturation [66]:

$$I_D = \frac{\sqrt{2}\beta\varepsilon_s}{2C_{0x}L_D}\left(\frac{kTn_i}{qN_{A,D}}\right)^2\sqrt{\frac{kT}{q\Psi_s}}\exp\left(\frac{q}{kT}\Psi_s\right), \quad (1)$$

where $\beta = W\mu C_{0x}/L_{eff}$ and $L_D = \sqrt{\varepsilon_s kT}/\sqrt{q^2 N_{A,D}}$ is the Debye length. In this equation C_{0x} is the oxide capacitance per unit area, k is the Boltzmann's constant, q is the absolute value of electron charge, T is the absolute temperature, n_i is the intrinsic carrier concentration, $N_{A,D}$ is the doping concentration, ε_s is the silicon permittivity, Ψ_s is the surface potential, μ is the carriers mobility, W is the channel width and L_{eff} is the effective channel length.

Regardless of the distribution within the substrate energy gap, interface traps are electrically neutral (total charge equals zero) when surface potential Ψ_s is equal to Fermi's potential ψ_F and that is the case when Fermi's level is in the middle of the semiconductor's energy gap. In that case, the shift between two subthreshold characteristics towards the V_G-axis is a consequence of the charge of FT only, and the gate voltage which

corresponds to these surface potential is denoted as V_{MG} (midgap voltage) and it can be obtained as abscissa of the (V_{MG}, I_{MG}) point at subthreshold characteristics (Fig. 3).

Using the equation $\log(I_D) = m \cdot V_G + n$, obtained by the linear fit of subthreshold characteristic, the V_{MG}, i.e., V_G that corresponds to $I_D = I_{MG}$ could be found as $V_{MG} = [\log(I_{MG}) - n]/m$. Using this procedure, V_{MG0} and V_{MG} are found. In Fig. 3 a region used for the linear fit is shown, and the straight lines obtained by the linear fits of subthreshold characteristics are extended up to corresponding midgap current I_{MG}.

The component of threshold voltage shift due to FT, ΔV_{ft} is

$$\Delta V_{ft} \equiv \Delta V_{MG} = V_{MG} - V_{MG0}, \tag{2}$$

where V_{MG0} and V_{MG} are midgap voltages before irradiation and after irradiation, respectively.

The component of threshold voltage shift due to ST, ΔV_{st}, is

$$\Delta V_{st} = (V_T - V_{MG}) - (V_{T0} - V_{MG0}) = V_s - V_{s0}, \tag{3}$$

where V_{T0} and V_T are transistors threshold voltages before irradiation and after irradiation, respectively and threshold voltage shift is $\Delta V_T = V_T - V_{T0}$. V_{T0} and V_T are determined from the transfer characteristics in saturation as the intersection between V_G-axis and extrapolated linear region of $\sqrt{I_D} = f(V_G)$ curves that are modeled by the following equation [66]:

$$I_D = \frac{\mu W C_{0x}}{2L_{eff}}(V_G - V_T)^2. \tag{4}$$

The total value of threshold voltage shift, ΔV_T can be expressed as [67]:

$$\Delta V_T = \Delta V_{ft} + \Delta V_{st}, \tag{5}$$

$$\Delta V_T = \pm \frac{q}{C_{0x}} \Delta N_{ft} + \frac{q}{C_{0x}} \Delta N_{st}, \tag{6}$$

where q is the absolute value of electron charge ΔN_{ft} is the areal density of FT and ΔN_{st} is the areal density of ST. Signs "+" and "-" are for p-channel and n-channel MOSFET, respectively. As it can be seen from exp. (6), both the FT and ST contribute to the threshold voltage shift in p-channel MOSFET in the same direction. Also, so called "rebound effect" [30] is absent in p-channel MOSFETs: this phenomenon is due to competitive effects to the positive charge in the oxide and negative interface traps generated in n-channel MOSFETs leading to a positive or negative ΔV_T values depending on the relatively values of ΔN_{ft} and ΔN_{st}. This is a reason that more commonly p-channel MOSFETs are used as sensor or dosimeter of ionizing radiation. It is emphasized that ΔN_{ft} could contain a small amount of SST that are located deeper in the oxide, since there is not enough time for the carriers from the channel to reach them during measurement frames.

3.2. Charge pumping technique

As opposed to the MG technique, the charge-pumping (CP) technique does not give changes in charge densities in the positive oxide trapped charge and interface traps, but is

used solely to determine interface traps density while the positive oxide trapped charge can be subsequently determined on the basis of the expression (6) under the condition that the change in threshold voltage known [68]-[70].

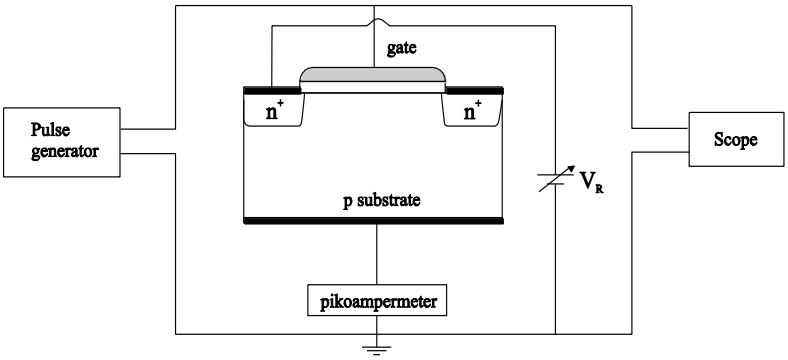

Fig. 4 Shematic diagram of charge pumping measurement.

The charge-pumping effect can be explained on the basis of the scheme in Fig. 4 [69]. The source and the drain of the transistor are short-circuited and *p-n* junction of source and drain with the substrate are inversely polarized with V_R voltage. In the absence of signal at the gate, under the influence of inverted polarization at the junction source-substrate and drain-substrate, the inverted saturation current of these connections will flow. When a train of rectangular pulses of sufficiently high amplitude is applied to gate (with pulse generator), a change of current direction in the substrate occurs. The intensity of that current is proportional with the pulse frequency, and "pumping" of the same amount of electric charge towards the substrate. As current cannot flow through oxide, the electric charge in the substrate go through *p-n* junction of source and drain. In this way, in the case of *n*-channel MOSFETs, a channel is formed under the gate in positive pulse half-period, whereby electrons are captured on interface traps. During the negative half-period, when the channel area turns into the state of accumulation, mobile electrons from the channel are returned to the source and drain, and the captured electrons are recombined with holes from the accumulated layer, thereby generating CP current I_{CP}, whose maximum value $I_{CP,\max}$ is expressed by[70]

$$I_{CP,\max} = fq^2 A_G \overline{D}_{it} \Delta\Psi_S = fqA_G \overline{D}_{it} \Delta E \,, \tag{7}$$

where A_G is the area under the gate active in charge pumping and f is the pulse frequency and $\Delta\Psi_S = q\Delta E$ is the total sweep of the surface potential that corresponds to the ΔE. In order to avoid recombination with channel electrons, it is necessary to ensure their return to the source and drain before overflow of cavities from the substrate occurs, which is accomplished by using reverse polarization of *p-n* junction or using a train of trapezoid pulses or triangular pulses with sufficient times for rise of time t_r and fall time t_f pulse. However, part of the electrons whose capture is shallowest, are in the meantime thermally emitted into conductive band of the substrate, reducing the width of interface traps energy range measure by the CP technique, so that CP current is generated by interface traps within the range [70]

$$\Delta E = -2kT \ln(v_{th} n_i \sqrt{\sigma_n \sigma_p} \frac{|V_T - V_{FB}|}{|\Delta V_G|} \sqrt{t_r t_f}) \tag{8}$$

which is 0.5 eV from the middle of the forbidden band. In the expression (8) v_{th} is thermal velocity, σ_n and σ_p are cross section surface of carrier captures, n_i is self-concentration of carriers in the semiconductor and ΔV_G is pulse height.

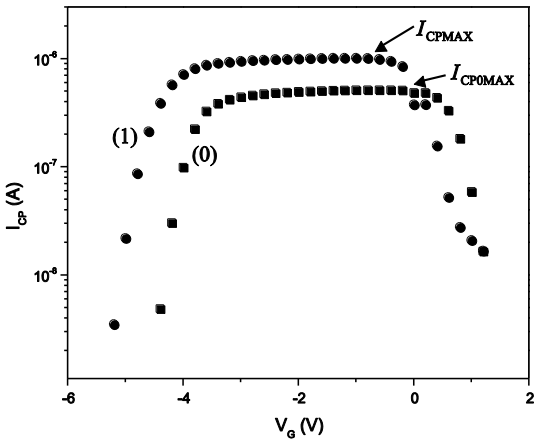

Fig. 5 Elliot-tipe CP curves of RADFETs with a 100 nm thick gate oxide manufactured by Tyndall National Institute, Cork, Ireland: (0) before gamma- ray irradiation and (1) after irradiation to 500 Gy.

The absolute value of interface traps density N_{it} can be calculated using equation (7) and $N_{it} = \overline{D}_{it} \cdot \Delta E$:

$$N_{it} = \frac{I_{CP\max}}{q \cdot A_G \cdot f}. \tag{9}$$

The change in areal density of interface traps is $\Delta N_{it}(CP) = N_{it}(t) - N_{it0}$, where $N_{it}(t)$ is the absolute value of interface trap density after irradiation time t and N_{it0} is the absolute value of interface trap density before irradiation. $I_{CP\max}$ (Fig. 5) is directly proportional to the pulse frequency and a small-size transistor with usual state density needs a frequency of at least several kHz to enable the charge-pumping current level reach the order of magnitude of picoampers. Due to this, CP measuring is most often conducted with frequencies in the range between 100 kHz and 1 MHz, whereby only FST (true interface traps) are registered (in some frequencies, CP is also contributed by of SST which also captures electrons from the channel [71]). As the CP technique required a separate outlet for the substrate, it could be concluded that it is not applicable for power VDMOSFETs, in which the *p*-bulk is technologically connected to the source. However the CP technique for these devices is applicable in a somewhat altered form (see [72], [73] for more details).

The density ΔN_{it} found by CP technique using expression (9) is, in fact, also the switching trap density $\Delta N_{st}(\text{CP}) \equiv \Delta N_{it}$ (CP). However, a very useful feature of the CP technique is that, as a much fast technique, it can sense only the FST and eventually just the fastest among SST. Hence, the density of ST measured by the CP technique is indicative of true interface trap (FST) behavior, i.e., $\Delta N_{st}(\text{CP}) = \Delta N_{fst}$. The simultaneous use of both techniques has a great advantage. For instance, the difference in the behavior of $\Delta N_{st}(\text{MG})$ and $\Delta N_{st}(\text{CP})$ is a consequence of SST [74], since $\Delta N_{st}(\text{MG}) = \Delta N_{sst} + \Delta N_{fst}$ and $\Delta N_{st}(\text{CP}) = \Delta N_{fst}$.

3.3. Single point threshold voltage shift measurements

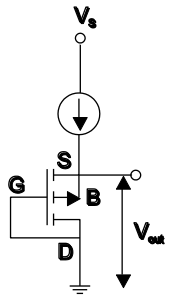

Fig. 6 Threshold voltage measurement configuration based on constant current.

As mentioned above, one of the methods for threshold voltage determination is based on transfer characteristics in saturation as the intersection between V_G-axis and extrapolated linear region of $\sqrt{I_D} = f(V_G)$ curves that are modeled by equation (4). The single point threshold voltage measurement requires measuring the drain-source voltage while the transistor remain biased by a constant drain current and the gate and drain terminals are short-circuited (Fig. 6) [75]. Under this configuration, the source-drain voltage shift is taken as ΔV_T. The monitoring of the drain-source voltage can be done continuously during irradiation.

Most of the commercial dosimetry systems based on MOSFETs measure increments of the drain-source voltage at constant drain current [76]-[78]. Usually, in the order to minimize the thermal drift, the drain current selected is the zero temperature coefficient current, I_{ZTC}, for which the thermal dependence of the drain-source voltage cancels out. When $I - V_{out}$ are measured at different temperatures, all of them intersect in the same point. In Fig. 7 presented the readout current ranging from 1 to 150 μA and the V_{out} voltage (V_{SD}) were measured at temperature ranges from 25 to 100 ^{o}C for RADFETs with 400 nm thick gate oxide manufactured by Tyndall National Institute, Cork, Ireland. As it can be seen, all of these curves intersected in the vicinity of 12 μA. It could be concluded that a selection of this current would minimize the effect of the temperature on the threshold voltage.

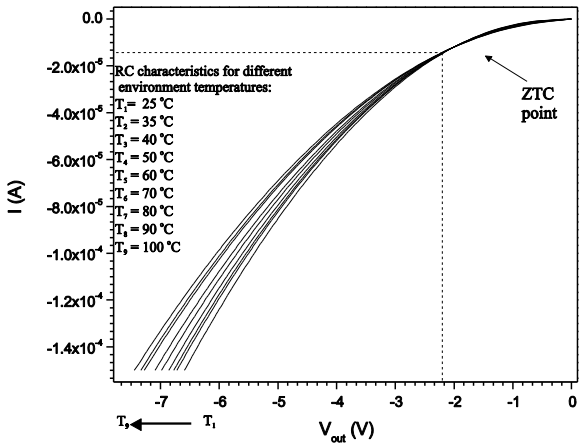

Fig. 7 Single-point characteristics of RADFETs with a 400 nm thick gate oxide layer manufactured by Tyndall National Institute, Cork, Ireland at various temperatures.

4. RADFET AS A SENSOR AND DOSIMETER OF IONIZING RADIATION

As it was stated before, the first results in MOSFETs application in dosimetry were published by Andrew Holmse-Siedle in 1974. [2]. Basic principles in application of these devices as sensors and dosimeters of ionizing radiation were presented. Several research groups which dealt with similar problems appeared afterwards. Those are Canadian research group [79], USA Navy research group [80], [81], French research group [82], [83], Netherlands [84], [85], USA [86], [87] and Serbia [88]-[90]. Large number of companies and institutes throughout the world are engaged in production of radiation sensitive MOSFETs. Among them is Tyndall National Institute, Cork, Ireland. This institute produces RADFETs with gate oxide thicknesses of 100 nm, 400 nm and 1 μm. Some of the results related to these components will be presented in this paper regarding several important dosimetric parameters.

4.1. Sensitivity of RADFETs irradiated by gamma rays

4.1.1. Influence of gate bias

Fig. 8 shows the threshold voltage shift ΔV_T of RADFETs with 100 nm gate oxide layer thickness for gamma-ray radiation dose D in the range from 100 to 500 Gy without and with gate bias during irradiation V_{irr} = 5V [91]. It can be seen that for irradiation without gate bias in the range from 0 to 500 Gy, ΔV_T increases for about 0.4 V. For the same dose interval, for gate bias 5 V, ΔV_T increased for about 2.3 V. The sensitivity is defined as $\Delta V_T / D$, so it can be concluded that the gate bias V_{irr} = 5V significantly increases the sensitivity of the RADFET.

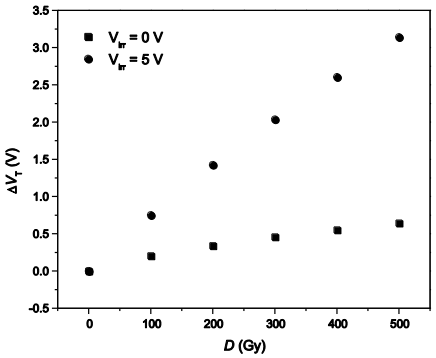

Fig. 8 Threshold voltage shift ΔV_T as a function of radiation dose D, for 100 nm gate oxide thick layer RADFETs, without and with gate bias during irradiation of V_{irr} = 5V.

In order to determine the contribution of FT and ST to total ΔV_T during irradiation, their densities were determined using MG and CP techniques, and results are presented in Figs. 9 and 10, respectively. It can be seen that the increase of radiation dose D lead to increase in both ΔN_{ft} and ΔN_{st} and that these increase are smaller for RADFETs previously irradiated without gate bias. Also, for the same values of D and V_{irr} the increase of FT density is larger than the increase of ST density. The ST density ΔN_{st} (MG) determined using MG technique is bigger than the ST density ΔN_{st} (CP) determined using CP technique. This is due to the fact that MG technique determines both SST and FST, while CP technique determines only FST (true interface traps). From Figs. 9 and 10, it can be seen that FT density is for about order of magnitude larger than ST density obtained using the MG technique. These results have shown that FT play a crucial role in threshold voltage shift.

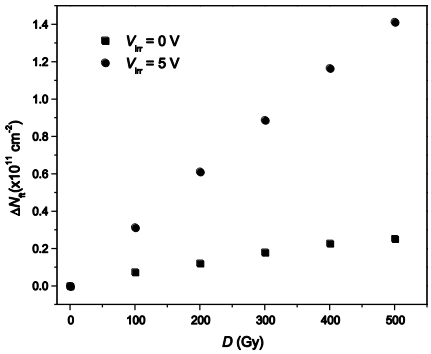

Fig. 9 The change in areal density of fixed traps ΔN_{ft} as a function of radiation dose D, for 100 nm gate oxide thick layer RADFETs, without and with gate bias during irradiation V_{irr} = 5V.

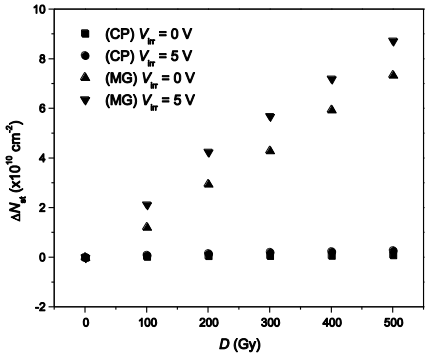

Fig. 10 The change in areal density of switching traps as a function of radiation dose *D*, for 100 nm gate oxide thick layer RADFETs, obtained by MG and CP technique without and with gate bias of V_{irr} = 5V.

Fig. 11 shows $\Delta V_T = f(D)$ dependence of a RADFETs with a gate oxide layer thickness of 100 nm for gamma-ray radiation dose in the range from 0 to 50 G [92]. During the irradiations the gate biases V_{irr} were 0, 1.25, 2.5, 3.75 and 5 V. The threshold voltage shift for the same dose increases in gate bias increase. The radiation dose up to 50 Gy did not degrade the linearity of the RADFETs significantly, which is significant for practical applications of these devices.

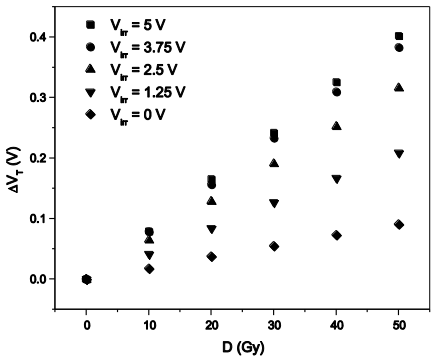

Fig. 11 Threshold voltage shift ΔV_T as a function of radiation dose *D* for RADFETs with a 100 nm thick gate oxide layer for various gate bias V_{irr} during irradiation.

In general, one can express the dependence of ΔV_T on *D* as:

$$\Delta V = A \cdot D^n , \tag{10}$$

where *A* is a constant and *n* is the degree of linearity. Ideally, *n* =1, and the dependence is linear with the sensitivity $S = \Delta V_T / D$. Correlation coefficients for linear fits for all values of V_{irr} (Fig. 11) are $r^2 = 0.999$. Having that r^2 are very close to one, it can be assumed that there is a linear dependence between ΔV_T and *D* and that the sensitivity of RADFETs for a given values of V_{irr} is the same in the range from 0 to 50 Gy.

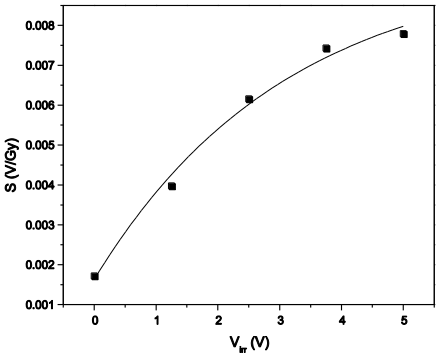

Fig. 12 Sensitivity S as a function of gate bias V_{irr} during irradiation for RADFETs with a 100 nm thick gate oxide layer for radiation dose of 50 Gy.

Fig. 12 shows the sensitivity S as a function of gate bias V_{irr} during gamma-ray radiation dose of 50 Gy for the RADFETs with 100 nm gate oxide thickness [92]. The symbols stand for experimental data while the solid lines represent fits, which are exponential.

Fig. 13 shows $\Delta V_T = f(D)$ of RADFETs with a 400 nm gate oxide layer thickness for gamma-radiation dose in range from 0 to 5 Gy and $V_{irr} = 0$V and $V_{irr} = 5$V [78], [93]. Expression (10) very well describes experimental data because the correlation coefficient is $r^2 = 0.999$. These results, as well as those presented in Figs. 8 and 12, show that the increase in gate bias during irradiation lead to the increase in ΔV_T value, i.e. the sensitivity is increased as well.

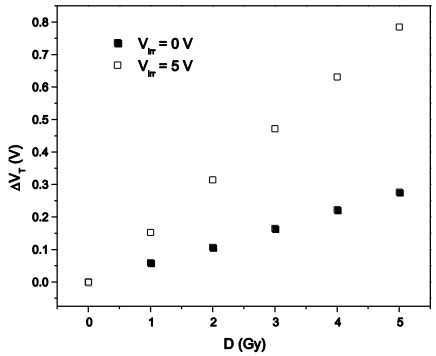

Fig. 13 Threshold voltage shift ΔV_T as a function of radiation dose D for RADFETs with a 400 nm thick gate oxide layer in the case without gate bias and gate bias of $V_{irr} = 5$V.

4.1.2. Influence of gate oxide layer thickness

Fig. 14 shows the threshold voltage shift ΔV_T as a function of radiation dose D for RADFETs with gate oxide layer thicknesses of 100 nm, 400 nm and 1μm. The gamma-ray irradiation of these devices was performed in the dose range from 0 to 50 Gy, while the gate bias was $V_{irr} = 5$V [92]. It can be seen that the increase in gate oxide layer

thickness lead to significant increase in ΔV_T for the same radiation dose. It is mainly due to the increase in FT density [94]. Experimental data fitting using expression (10) for n=1, gives the correlation coefficient value, for RADFETs whith 100 and 400 nm gate oxide thickness, $r^2 = 0.999$, what proves linear dependence between ΔV_T and D, i.e. the sensitivity is the same in considered dose range and this value is higher for 400 nm gate oxide later thickness. For 1 μm gate oxide thickness RADFETs, correlation coefficient is $r^2 = 0.976$, so there is no linear dependence between ΔV_T and D, and hence the sensitivity is different for different values of radiation dose.

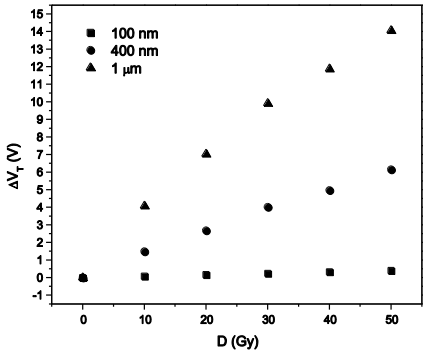

Fig. 14 Threshold voltage shift ΔV_T as a function of radiation dose D for three values of gate oxide layer thickness. Gate bias during irradiation was V_{irr} = 5V.

$\Delta V_T = f(D)$ dependence for RADFETs with a gate oxide layer thicnesses of 400 nm and 1μm is shown in Fig. 15 [78]. Irradiation of these devices was also performed with gamma-rays and gate bias during irradiation of V_{irr} = 5V but the dose range was from 0 to 5 Gy. I was also shown that the sensitivity increases with gate oxide thickness and that here is linear dependence between ΔV_T and D (correlation coefficient $r^2 = 0.999$).

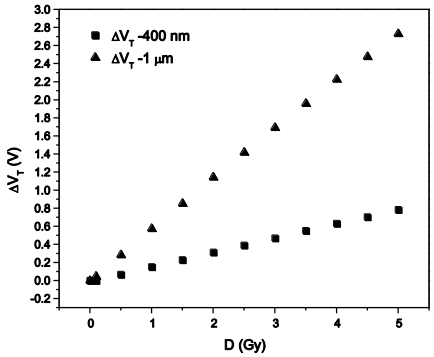

Fig. 15 Threshold voltage shift ΔV_T as a function of radiation dose D for two values of gate oxide layer thickness. Gate bias during irradiation was V_{irr} = 5V.

4.1.3. Photon energy influence on RADFETs sensitivity

Threshold voltage shift ΔV_T for RADFETs with 1 μm gate oxide layer thickness, irradiated with gamma-rays which originates from ^{60}Co and X-rays with energy of 140 keV for radiation dose in the range from 0 to 5 Gy for V_{irr} = 0V and V_{irr} = 5V is presented in Figs. 16 and 17, respectively [95]. It can be seen that ΔV_T increases in much higher in the case when RADFETs are irradiated with X-rays then in the case of gamma-rays. It is a consequence of different photon energies which lead to ionization of the oxide gate molecules. Namely, X-rays photon energy of 140 keV leads to molecule ionization by both photoeffect and Compton's effect, while gamma-rays, which originate from ^{60}Co with energies of 1.17 and 1.33 MeV lead to molecules ionization only by Compton's effect [31]. Since the probability for molecule ionization by photoeffect is significantly higher than Compton's effect, during X-ray irradiation a large number of FT and ST are formed than during gamma-ray irradiation which directly causes the change in ΔV_T values.

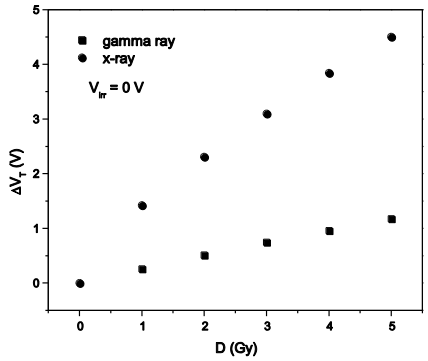

Fig. 16 Threshold voltage shift ΔV_T as a function of radiation dose of gamma and X-ray *D* for 1 μm gate oxide thick layer RADFETs irradiated without gate bias.

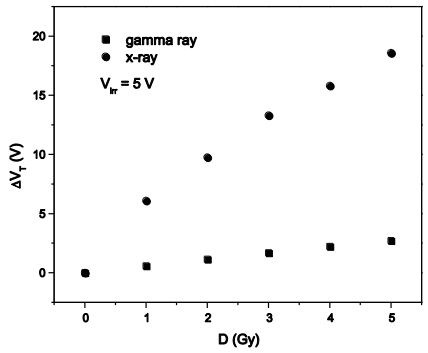

Fig. 17 Threshold voltage shift ΔV_T as a function of radiation dose of gamma and X-ray *D*, for 1 μm gate oxide thick layer RADFETs irradiated with V_{irr} = 5V.

Fitting of experimental data for gamma radiation dose in the range from 0 to 5 Gy (Figs. 16 and 17) using the expr. (10) for n=1 gives correlation coefficient of $r^2 = 0.998$ for both $V_{irr} = 0$V and $V_{irr} = 5$V. Having that the correlation coefficients are very close to one, it can be assumed that there is a linear dependence between ΔV_T and D, so that the sensitivity ΔV_T / D is the same in whole interval. Correlation coefficients for the case when RADFETs are irradiated with X-rays (Figs. 16 and 17) are 0.96 and 0.95 for $V_{irr} = 0$V and $V_{irr} = 5$V, respectively, so it is shown that there is no linear dependence between ΔV_T and D.

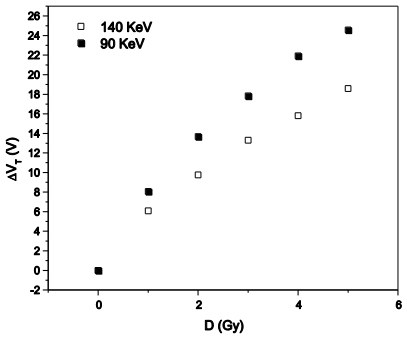

Fig 18 Threshold voltage shift ΔV_T as a function of radiation dose D, for 1 μm gate oxide thick layer RADFETs, for two value of energy of X-ray. Gate bias during irradiation is $V_{irr} = 5$V.

Fig. 18 shows $\Delta V_T = F(D)$ dependence of RADFETs with 1 μm gate oxide layer thikcness during X-ray irradiation with photons energies of 90 and 140 keV for gate bias $V_{irr} = 5$V [96]. It can be seen that lower photon energy leads to a greater change in ΔV_T for the same radiation dose. Similar behavior is detected in TN-502 RDI MOSFETs (Thomson and Neilson Electronic Ltd, Ottawa, Canada) [97].

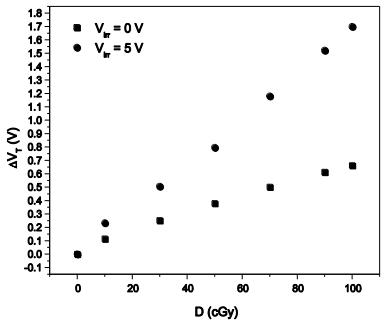

Fig. 19 Threshold voltage shift ΔV_T as a function of X-ray radiation dose D for RADFETs with a 400 nm thick gate oxide layer. Radiation was performed without and with gate bias of $V_{irr} = 5$V.

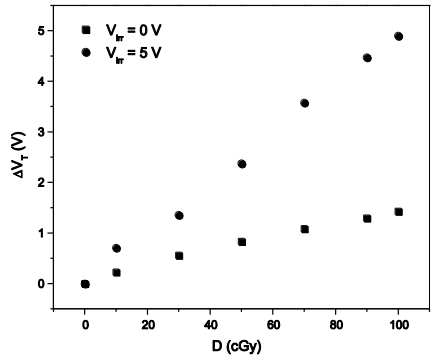

Fig 20 Threshold voltage shift ΔV_T as a function of X-ray radiation dose D for RADFETs with a 1μm thick gate oxide layer. Radiation was performed without and with gate bias of V_{irr} = 5V.

Figs. 19 and 20 show the threshold voltage shift for X-ray radiation dose in the range from 0 to 100 cGy for RADFETs with gate oxide layer thickness of 400 nm and 1 μm, respectively. Fig. 21 shows the same dependence for X-ray radiation dose in the range from 1 to 10 cGy for RADFETs with gate oxide layer thickness of 1 μm [98]. These dependence are given for gate bias during irradiation V_{irr} = 0V and V_{irr} = 5V. As it can be seen, ΔV_T values are higher when the gate bias during irradiation was V_{irr} = 5V, compared with the case when it was V_{irr} = 0V. Furthermore, ΔV_T is higher for RADFETs with large gate oxide layer thickness (Figs. 19 and 20). Results presented in Fig. 21 show that ΔV_T values can be detected with good reliability even for radiation dose of 1 cGy.

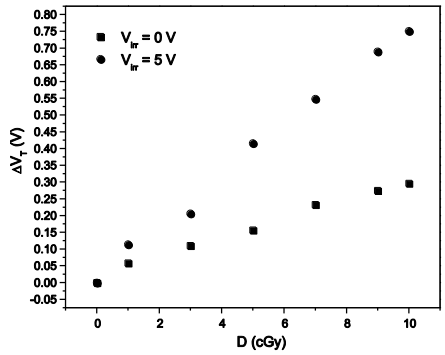

Fig. 21 Threshold voltage shift ΔV_T as a function of X-ray radiation dose D for RADFETs with a 1μm thick gate oxide layer. Radiation was performed without and with gate bias of V_{irr} = 5V.

4.2. Irradiated RADFETs fading

As a dosimeter a RADFETs must satisfied two fundamental dosimetric demands: a good compromise between sensitivity to irradiation and stability with time after irradiation. The stability means insignificant change in ΔV_T of an irradiate RADFET at room temperature for a long period of time, i.e., dosimetric information should be saved for a long period. There are two important reasons for this: first, being the fact that the dose cannot always be acquired immediately after irradiation, but after a certain period of time; second, as by individual monitoring, the exact moment of irradiation is often unknown, and the radiation dose measurements are performed periodically. Room temperature stability of irradiated RADFET can be followed by calculating fading F, which can be calculated as [95]:

$$F = \frac{V_T(0) - V_T(t)}{V_T(0) - V_{T0}} \cdot 100\ [\%] = \frac{V_T(0) - V_T(t)}{\Delta V_T(0)} \cdot 100\ [\%]\,. \tag{11}$$

where V_{T0} is the pre irradiation threshold voltage, $V_T(0)$ is the threshold voltage immediately after irradiation, $V_T(t)$ is the threshold voltage after annealing time t and $\Delta V_T(0)$ is the threshold voltage shift immediately after irradiation.

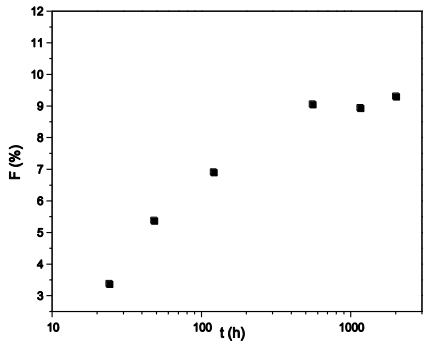

Fig. 22 Fading F at room temperature for 2000 h of RADFETs with a 400 nm thick gate oxide layer previously irradiated with gamma-ray radiation dose 5 Gy.

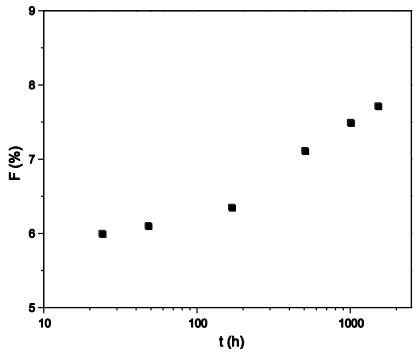

Fig. 23 Fading F at room temperature for 2000 h of RADFETs with a 400 nm thick gate oxide layer previously irradiated with gamma-ray radiation dose 50 Gy.

Fading RADFETs with gate oxide layer thickness of 400 nm which were previously irradiated with 5 Gy gamma-rays are shown in Fig. 22. It can be seen that fading for the first 24 h annealing at room temperature is about 3.5% while for the annealing time from 24 h to 800 h it is increases for about 6%. During further annealing fading is insignificant. For the same type of RADFETs previously irradiated with 50 Gy gamma-rays is shown in Fig. 23. It can be seen that for the first 24 h annealing at room temperature fading is about 6% and its value slightly increases to 200 h annealing time. For annealing time longer than 200 h comes to a slight increase in fading, and therefore, is fading after 2000 h for about 2% higher than after 200 h.

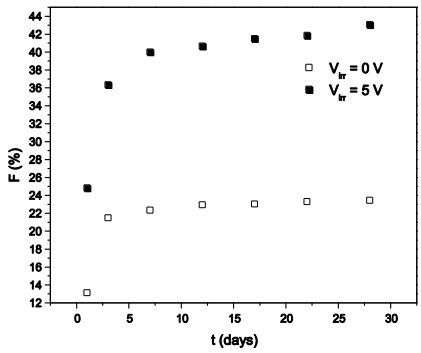

Fig. 24 Fading *F* at room temperature for 2000 h of RADFETs with a 400 nm thick gate oxide layer previously irradiated with X-ray radiation dose 100 cGy.

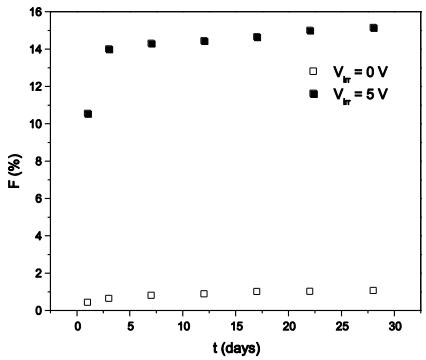

Fig. 25 Fading *F* at room temperature for 28 d of RADFETs with a 1μm thick gate oxide layer previously irradiated with X-ray radiation dose 100 cGy.

Fading results for RADFETs with gate oxide thickness of 400 nm and 1 μm, at room temperature previously irradiated with X-rays up to 100 cGy, are presented in Figs. 24 and 25, respectively [98]. In Fig. 26 fading of RADFETs with gate oxide layer thickness of 1 μm previously irradiated with X-rays up to 10 cGy is also presented [98]. Fading of RADFETs with gate oxide layer thickness of 400 nm, which were irradiated with gate bias of 5 V, is 40% in the first 7 d, whereas those of RADFETs irradiated without gate

bias during irradiation have 22% fading also in the first 7 d (Fig. 24). For the time period between 7 and 28 d, fading of RADFETs irradiated with gate bias 5 V increased for about 3% whereas that of RADFETs irradiated without gate bias during irradiation fading had a nearly constant value. Fading of 1μm thick gate oxide layer RADFETs, which were irradiated up to 100 cGy with gate bias 5 V in the first 7 d was 14% (Fig. 25), whereas for the time period between 7 and 28 d, it increases about 1%. RADFETs with the same gate oxide layer thickness, which were irradiated without gate bias the first 7 d, have a fading increase for about 1% and this value is kept up to 28 d.

Figs. 24 and 25 show that fading is lower when the gate oxide layer of RADFETs is thicker which in accordance with early study [10], [89], showed that fading decreases with the increase in gate oxide thickness.

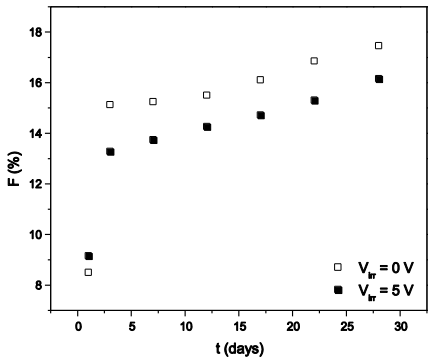

Fig. 26 Fading *F* at room temperature for 28 d of RADFETs with a 1μm thick gate oxide layer previously irradiated with X-ray radiation dose 10 cGy.

In RADFETs with gate oxide layer thickness of 1μm irradiated up to 10 cGy, the highest fading occurs in the first 3 d and it is 15% for RADFETs irradiated without gate bias and 13% for RADFETs with 5 V gate bias during irradiation (Fig. 26). Moreover, in both case, fading from 3 to 28 d is smaller than 2%.

Fading of RADFETs is mainly a consequence of positive oxide trapped charge decrease. This decrease is a consequence of electrons tunneling from Si into SiO_2; these electrons are captured at positive oxide trapped charge, which leads to their neutralization/ compensation, and thus instability of manifested threshold voltage shift [99].

4.3. The possibility of RADFETs re-use

Many investigations have showed that RADFETs cannot be used for subsequent determination of ionizing radiation dose. Namely, these dosimeters are only used to measure the maximum dose, which is determined by the type and sensitivity of RADFET. When the maximum radiation dose is reached, these RADFETs should be replaced. The first results dealing with the possibility of re-use of these devices are given in ref. [10] for radiation dose 400 Gy. Later investigations for the same components are presented in [23], [100]. Irradiation was performed with gamma-rays up to 35 Gy, without gate bias and with gate bias V_{irr} = 2.5V and V_{irr} = 5V. Fig. 27 shows the threshold voltage shift ΔV_T

as a function of radiation dose *D*, for both the first and second irradiation with gate bias of V_{irr} = 5V. After the first irradiation, the RADFETs were annealed at room temperature for 5232 h without gate bias. After this, the annealing process was continued at 120 °C without gate bias for 432 h. The RADFETs were then irradiated under the same conditions. The values of ΔV_T during the first and second irradiation is very close. Such results are in oposition with earlier results [10] where it was shown that values for ΔV_T during the first irradiation are higher than the values obtained during the second irradiation.

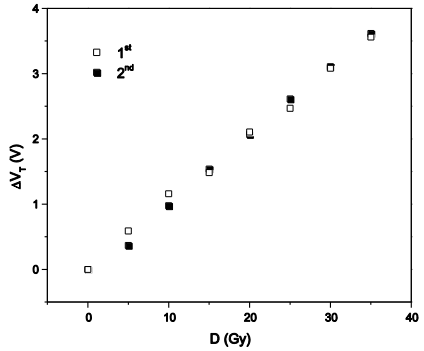

Fig. 27 Threshold voltage shift ΔV_T as a function of radiation dose *D* of RADFETs with a 400 nm thick gate oxide layer for both the first and second irradiation with gate bias of V_{irr} = 5V.

The first and second irradiation of RADFETs lead to approximately the same increase of ΔN_{ft} (Fig. 28) while the increase of ΔN_{st} (MG) is higher during the second irradiation (Fig. 29). ΔN_{fst} (CP) is higher during the second irradiation (Fig. 30). On the basis of the results presented in Figs. 28, 29 and 30 it can be seen that the major contribution to ΔV_T increase during the first and second irradiation originates from FT, which density is an order magnitude higher than ST(MG) density for a radiation dose of 35 Gy.

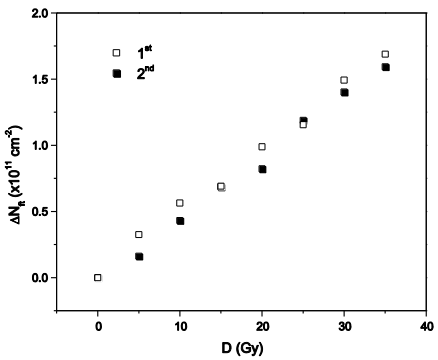

Fig. 28 Areal density of fixed traps ΔN_{ft} as a function of radiation dose *D* of RADFETs with a 400 nm thick gate oxide layer for both the first and second irradiation with gate bias of V_{irr} = 5V.

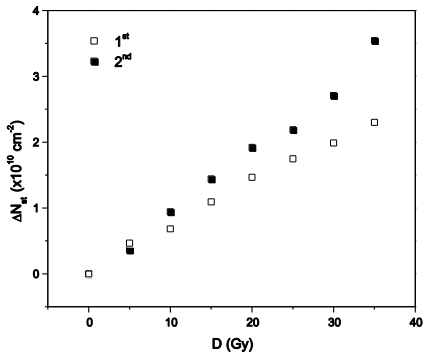

Fig. 29 Areal density of switching traps ΔN_{st} (MG) as a function of radiation dose D of RADFETs with a 400 nm thick gate oxide layer for both the first and second irradiation with gate bias of V_{irr} = 5V.

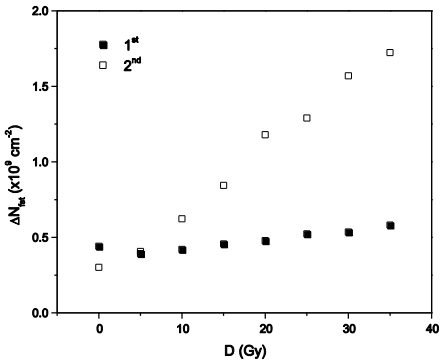

Fig. 30 Areal density of switching traps ΔN_{st} (CP) as a function of radiation dose D of RADFETs with a 400 nm thick gate oxide layer for both the first and second irradiation with gate bias of V_{irr} = 5V.

5. LOW-COST COMMERCIAL P-CHANNEL MOSFET AS A RADIATION SENSOR

In recent years, many investigations are driven toward applications of low-cost commercial p-channel MOSFETs as a radiation sensors in radiotherapy [101]. Paper [102] presents results of some most important dosimetric parameters (sensitivity, linearity, reproductibility and angular dependence) for power p-channel MOSFETs 3N163. These transistors were irradiated by gamma rays from ^{60}Co up to 55 Gy. These devices were irradiated without gate bias. Fig 31 shows the threshold voltage shift ΔV_T versus radiation dose D for 15 devices. As expected, the ΔV_T values increases when the radiation dose in MOSFETs increases. The data show excellent linearity with a mean sensitivity value of 29.2 mV/Gy and resonable good reproducibility up to a total dose of 58 Gy (which is around to the total dose used in typical radiotherapy treatments). Moreover, the angular and dose-rate dependencies are similar to those of other, more specialised p-channel MOSFETs (RADFETs). Authors of this paper concluded that power

p-channel MOSFET 3N163 would be an excellent candidate as a sensor of a low-cost system capable of measuring the gamma radiation dose. This radiation sensor could be placed on patient without the need for wires, and the threshold voltage shift, which is indicative of the radiation dose could be measured after the completion of each irradiation session with a resonable degree of confidance.

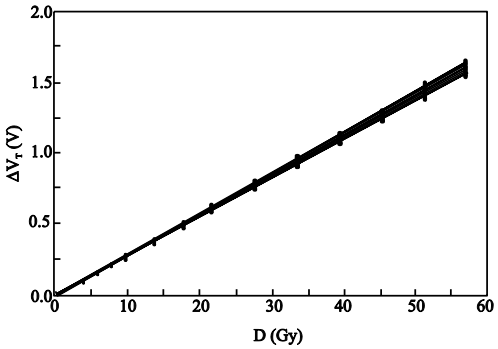

Fig. 31 Threshold voltage shift ΔV_T as a function of radiation dose D for fifteen MOSFETs 3N163 irradiated with gamma-rays without gate bias.

Martines-Garicia et al [103] investigatted the possibility of vertical diffusion MOS, also called double-diffused MOS transistor, or simply DMOS, as a sensor of ionizing radiation. Those components were DMOS BS250F, ZVP3306 and ZVP4525, manufacured by Diodes Incorporated (Plano, USA). The irradiation was performed by an electron beam of 6 MeV energy without gate bias. The same auhors invesigated the behavior of p-channel MOS transistors from integrated circuis CD4007 (Texas Instruments, Dallas, USA and NXP Semiconductors, Eindhoven, Netherlands) under 6 MeV energy electron beam. In Fig. 32 the ΔV_T versus D is ploted for four simples of the ZVP3306 DMOS transistors. The results for the other models DMOS transistors are similar. As it can be seen there is a linear dependence betveen ΔV_T and D to radiation dose of 25 Gy. Values of sensitivity for BS250F, ZVP4525 and ZVP3306 are 3.1, 3.4 and 3.7 mV/Gy, respectively.

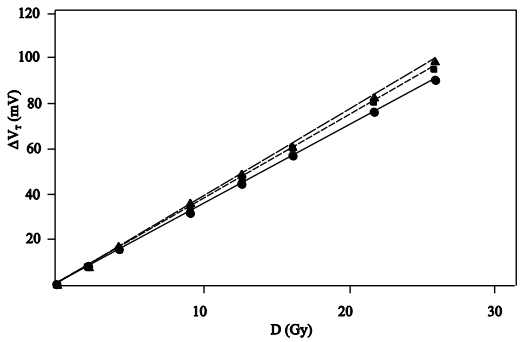

Fig. 32 Threshold voltage shift ΔV_T as a function of radiation dose D for four DMOD ZVP3306 irradiated with 6 MeV electrons without gate bias.

It is shown [103] that p-channel MOS transistors from integrating circuits CD4007 in unbiased configuration during irradiation showed the sensitivity 4.6 mV/Gy with a very good linear behaviour of the threshold voltage shift versus radiation dose. As the thermal compensation may be applied this transistor may be considered as a promising candidate to use as dosimeter in intra-operative radiology.

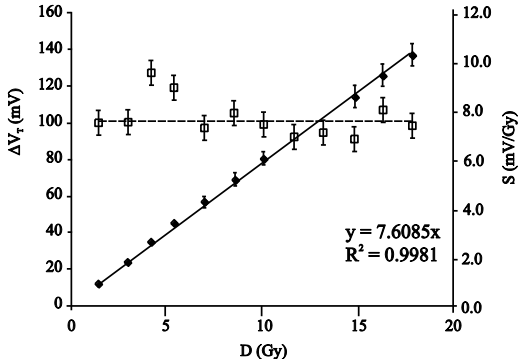

Fig. 33 Threshold voltage shift ΔV_T and sensitivity S as a function of radiation dose D for p-channel MOS transistors from integrated circuits CD4007 irradiated with 6 MeV electrons with gate bias V_{irr} = 0.6V.

Fig. 33 shows the $\Delta V_T = f(D)$ dependence when CD4007 manufactured by Texas Instruments irradiated with electron beam of 6 MeV. During irradiation gate bias is 0.6 V. The data present a linear behaviour showing that p-chnnel transistors from this integrating circuit is suitable foR electron beam dosimetry because the sensitivity is 7.4 mV/Gy. Sensitivity for CD4007 manufactured by NXP Semiconductor for the same conditions is 8.9 mV/Gy.

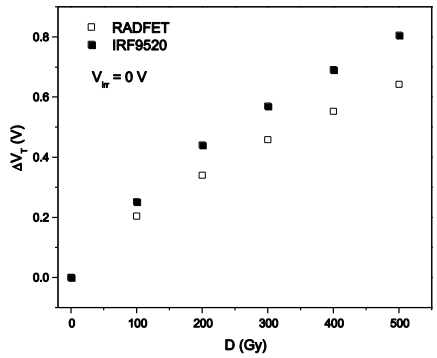

Fig. 34 Threshold voltage shift ΔV_T as a function of radiation dose D for RADFETs and VDMOSFETs IRF9520 irradiated without gate bias.

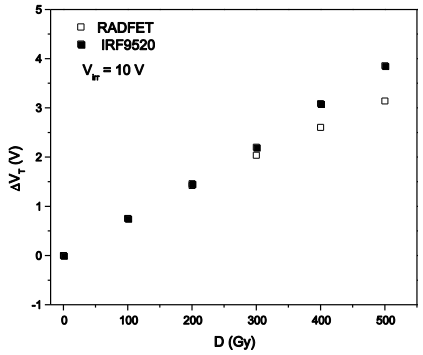

Fig. 35 Threshold voltage shift ΔV_T as a function of radiation dose D for RADFETs and VDMOSFETs IRF9520 irradiated with gate bias of V_{irr} = 10V.

A comparative study of RADFETs manufactured by Tyndall National Institute, Cork, Ireland with 100 nm gate oxide layer thicknes and commercial p-channel power VDMOSFETs IRF9520 manufactured by International Rectifier sensitivity to gamma-ray irradiation in the dose range from 0 to 500 Gy is given in paper [104]. Figs. 34 and 35 show the dependence between ΔV_T and D for RADFETs and IRF9520 in the case when they were irradiated without gate bias (V_{irr} = 0V) and with gate bias of V_{irr} = 10V, respectively. It can be seen that ΔV_T is higher for IRF9520 then for RADFET for the same radiation dose. The difference in ΔV_T is probably a concequence of different technological procedures during device fabrication. It is shown that linear dependence between ΔV_T and D valid only for devices with V_{irr} = 10V during irradiation (the value of corelation coefficient obtained by experimental data fiting using expression (10) is r^2 = 0.998).

Figs. 36 and 37 present the change in areal densities of FT, ΔN_{ft} for RADFET and IRF9520 without gate bias and with gate bias V_{irr} = 10V during irradiation, respectively [104]. It can be seen that ΔN_{ft} is larger in IRF9520 then in RADFET as well as that gate bias leads to the increase in ΔV_T for the same value of radiation dose for both types of transistors.

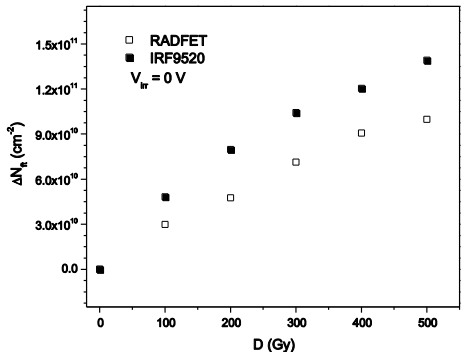

Fig. 36 The change in areal density of FT ΔN_{ft} as a function of radiation dose D for RADFETs and VDMOSFETs IR9520 irradiated without gate bias.

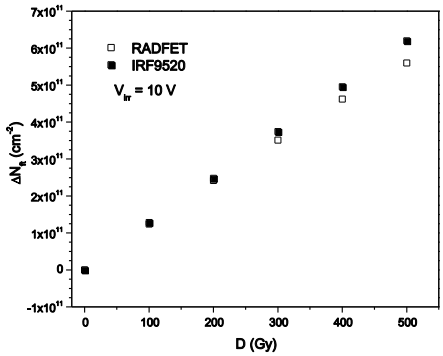

Fig. 37 The change in areal density of FT ΔN_{ft} as a function of radiation dose D for RADFETs and VDMOSFETs IR9520 irradiated with gate bias of V_{irr} = 10V.

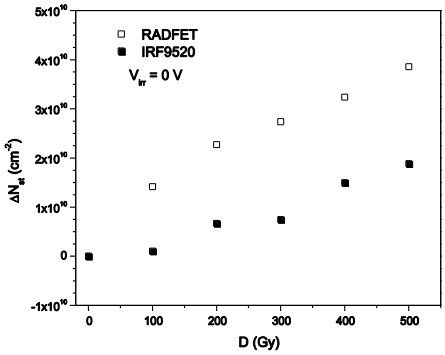

Fig. 38 The change in areal density of ST ΔN_{st}, determined using MG technique, as a function of radiation dose D for RADFETs and VDMOSFETs IR9520 irradiated without gate bias.

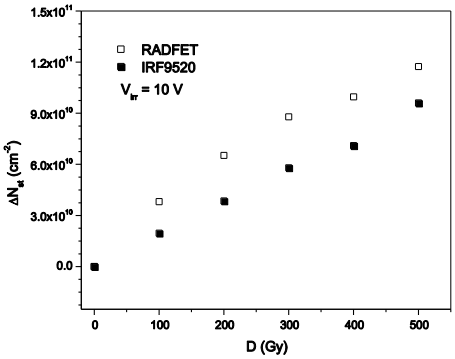

Fig. 39 The change in areal density of ST ΔN_{st}, determined using MG technique, as a function of radiation dose D for RADFETs and VDMOSFETs IR9520 irradiated with gate bias of V_{irr} = 10V.

The change in areal densities of ST, ΔN_{st} determined by MG technique for RADFET and IRF9520 without gate bias and with V_{irr} = 10V gate bias are presented in Figs. 38 and 39, respectively [104]. It can be seen that ΔN_{st} is smaller in IRF9520 than in RADFET. However, ΔN_{ft} is considerably larger than ΔN_{st} in both types of devices. On the basis of these data it can be concluded that ΔN_{ft} predominantly contributes to ΔV_T increase during irradiation.

Fading of irradiation IRF9520 and RADFET up to 500 Gy is calculated 24 h after irradiation using equat. (11). For this time the device were kept at room temperature without gate bias. It was shown that the fading is higher in IRF9520 than in RADFETs and it is smaller for devices previously irradiated with gate bias V_{irr} = 10V.

6. CONCLUSION

Intensive investigations of radiation sensitive MOSFETs (RADFETs) have been performed in order to investigate their application in dosimetry. Their relatively small volumen give them advantage over some other dosimetric systems, which is particulary important in in-vivo dosimetry as well as in control of gradient radiation fielld of x-rays. RADFETs are most commonly used for photon and ionizing radiation charged particles detection. It can be also used for neutron detection, but their sensitivity is much smaller than for photons and charged particles. Their sensitivity can be increased by gate bias application during irradiation and by increasing the gate oxide layer thickness. The sensitivity increases with the decrease in ionizing radiation photon energy. It is required for these components to achieve minimal variation in threshold voltage shift after irradiation at room temperature, i.e. it is neccessary to preserve the dosimetric information for a long period of time. Considered RADFETs are sensitive sensors of gamma and x-rays, because they can register doses below 1 cGy. Unfortinatelly, their major disadvantage is large fading immidiatelly after irradiation. Investigations in the past few years have shown that some commercially available p-channel MOSFETs can be very efficiently applied as gamma and x-ray sensors as well as electrons sensors with energyes of seweral MeV. Those are low power p-channal MOSFETs 3N163, DMOS BS250F, ZVP3306, ZVP4525 and power VDMOSFETs IRF9520. Furthermore, p-channel MOS transistors, for example from CD4007, can be used as sensors of ionizing radiation.

Acknowledgement: *The paper is a part of the research done within the project supported by the Ministry of Education, Science and technological Development of the republic of Serbia under project no. 32026.*

REFERENCES

[1] W. Poch and A.G. Holmes-Siedle, „The mosimeter- a new instrument for measuring radiation dose“, *RCA Eng.*, vol. 16, pp. 56-59, 1970.

[2] A. G. Holmes-Siedle, „The space charge dosimeter-general principles of a new method of radiation dosimetry“, *Nucl. Instrm. Methods*, vol. 121, pp. 169-179, 1974.

[3] L. Adams and A. Holmes-Siedle, „The development of MOS dosimetry unit for use in space“, *IEEE Trans. Nucl. Sci.*, vol. 18, pp. 1607-1612, 1978.

[4] R. R. Price, C. Benson an K. Rodgers, „Development of RadFET linear array for intracavitary in vivo dosimetry in external radiotherapy and brachyterapy“, *IEEE Tran. Nucl. Sci.*, vol. 51, pp. 1420-1426, 2004.

[5] R. Ramasechum, K.S. Kulli, T.J. Zhang, B. Norling, A. Hallil and M. Islam, „Performance characteristics of a micro MOSFET as an in vivo dosimeter in radiation therapy“, *Phys. Med. Biol.*, 49, pp. 4031-4048, 2004.
[6] G. Tarr, K. Shortt, Y. Wang and I. Thomson, „A sensitive temperature-compensated, zero-bias floating gate MOSFET dosimeter“, *IEEE Trans. Nucl. Sci.*, vol. 51, pp. 1277-1282, 2004.
[7] M. C. Lavallee, L. Gingras and B. Luc, „Energy and interated dose dependence of MOSFET dosimeter sensitivity for irradiation eneries between 30 kV and ^{60}Co“, *Med. Phys.*, vol. 33, pp. 3683-3689, 2006.
[8] R. Kohuo, T. Nishio, T. Miyagishi, E. Hirano, K. Hotta, M. Kowashima and T. Ogino, „Experimental evaualation of a MOSFET dosimeter for proton dose measurements“, *Phys. Med. Biol.*, vol. 51, pp. 6077-6086, 2006.
[9] A. Holmes-Siedle and L. Adams, „RADFETs: a review of the use of metal-oxide silicon devices as integrating dosimeters“, *Rad. Phys. Chem.*, vol. 28, 224-235, 1986.
[10] A. Kelleher, N. McDonnell, B. O'Neill, W. Lane, L. Adams, „Investigation into the re-use of pMOS dosimeter“, *IEEE Trans. Nucl. Sci.*, vol. 41, pp. 445-451, 1994.
[11] L. Z. Scheick, P.J. McNulty and D.R. Roth, „Dosimetry based on the erasure of floating gates in natural radiation environments“, *IEEE Trans. Nucl. Sci.*, vol. 45, pp. 2681-2688, 1998.
[12] K. Kay, E. Mullen, W. Stapor, R. Circle and P. McDonald, „GRRES dosimetry results and comparison using the space radiation dosimeter and p-channel MOS disieteter“, *IEEE Tran. Nucl. Sci.*, vol. 39, pp. 1846-1850, 1992.
[13] A. Faigon, J. Lipovetzky, E. Redin and G. Kruscenski, „Expresion of measurement range of MOS dosimeters using radiation induced charge neutralization“, *IEEE Trans. Nucl. Sci.*, vol. 55, pp. 2141-2147, 2008.
[14] B. O'Connell, C. Connely, C. McCarthy, J. Doyle, W. Lane and L. Adams, „Electrical performance and irradiation sensitivity of stacked pMOS dosimeters under bulkbias control“, *IEEE Trans. Nucl. Sci.*, vol. 45, pp. 2689-2694, 1988.
[15] G. Sarrabayrouse, Buchdahl, V. Poliscuk and S. Siskos, „Stacked-MOS ionizing radiation dosimeters: Potentials and limitations, *Radiat. Phys. Chem.*, vol. 71, pp. 737-739, 2004.
[16] R.C. Hughes, D. Huffman, J.V. Snelling, T.E. Zipperian, A.J. Ricoo and C.A. Kelsey, „Miniature radiation dosimeter for in vivo radiation measuremnts“, *Int. Rad. Oncol. Biol. Phys.*, vol. 14, pp. 963-967, 1988.
[17] D.J. Gladstone, X.Q. Lu. J.L. Humm, H.F. Bowman and L.M. Chin, „A miniature MOSFET radiation probe“, *Med. Phys.*, vol. 21, pp. 1721-1728, 1994.
[18] G.I. Kaplan, A.B. Rosenfeld, B.J. Allen, J.T. Booth, M.G. Carolan and A. Holmes-siedle, „A special resolution by MOSFET dosimetry of an x-ray microbeam“, *Med. Phys*., vol. 27, pp. 239-244, 2000.
[19] G. Sarabayrouse and V. Polischuk, „MOS ionizing radiation dosimeters: from low to high dose measurement“, *Radiat. Phys. Chem*., vol. 61, pp. 511-513, 2001.
[20] A. Jaksić, G. Ristić, M. Pejović, A. Mohammadzadeh, C. Sudre and W. Lane, „Gamma-ray irradiation and post-irradation response of high dose range RADFETs“, *IEEE Trans. Nucl. Sci*., vol. 49, pp. pp. 1356-1363, 2002.
[21] R. A. Price, „Towards and optimum design of a P-MOS radiation detector for use in high-energy medical photon beams and neutron facilities: analysis of activation materials“, *Radiation Protection Dosimetry*., vol. 115, pp. 386-390, 2005.
[22] M. M. Pejović, M.M. Pejović, A.B. Jakšić, K.Dj. Stanković and A.A. Marković, "Successive gamma-ray irradiation and Corresponding post-irradiation annealing of PMOS dosimeters", *Nucl. Technol. and Radiat. Protection*, vol. 27, pp. 341-345, 2012.
[23] M. M. Pejović, M.M. Pejović and A.B. Jakšić, „Contribution of fixed oxide traps to sensitivity of PMOS dosimeters during gamma ray irradiation and annealing at room and elevated temperature", *Sensors and Actuators A*, vol. 174, pp. 85-90, 2012.
[24] S. Alshaikh, M. Carolan, M. Petasecca, M. Lerch and A.B. Metealfe, „Direct and pulsed current annealing of p-MOSFET based dosimeter, the MOSkin“, *Australs Phys. Eng. Sci. Med.*, vol. 37, pp. 311-319, 2014.
[25] G-Wen Luo, Qi. Z.-Y. Deng, A. Rosenfeld and W- X?, „Investigated of a pulsed current annealing method in reusing MOSFET dosimeters for in vivo IMRT dosimetry“, *Med. Phys.*, vol. 41, 0511710, 2014.
[26] G. Ristić, S. Golubović and M. Pejović, „pMOS dosimeter with two-layer gate oxide operated at zero negative bias", *Electr. Lett.*, vol. 30, pp. 295-296, 1994.
[27] G. Ristić, A. Jakšić, M. Pejović, "pMOS dosimetric transistors with two-layer gate oxide", *Sensors and Actuators A*, vol. 63, pp. 129-134, 1997.

[28] G. Sarrabayrouse and F. Gessinn, "Thick oxide MOS trnsistors for ionizing radiation dose measurement", *radioprotection*, vol. 29, pp. 557-572, 1994.
[29] A. Haran, A. Jakšić, N. Rafaeli, A. Elyahu, D. David and J. Barak, *IEEE Trans. Nucl. Sci.*, vol. 51, 2917-2921, 2004.
[30] T. P. Ma and P.V. Dressendorfer, *Ionizing Radiation Effects in MOS Devices and Circuits*, New York: Willey and Sons, 1989.
[31] G. S. Ristić, "Influence of ionizing radiation and hot carrier injection on metal-oxide-semiconductor transistors", *J. Phys. D: Appl. Phys.*, vol. 41, 023001 (19 pp), 2008.
[32] M. Pejović, P. Osmokrović, M. Pejović and K. Stanković, "Influence of ionizing radiation and hot carrier injection on metal-oxide-semiconductor transistors". In M. Nenoi (Ed), *Current Topic in Radiation Research*. INTECH. Institute for New Technologies, Maastricht (NL), Chapter 33, <http://www.intechopen.com/books/current-topics-in-ionizing-radiation-research>. OCLC: 846871029, 2012.
[33] C. T. Sah, "Origin of interface states and oxide charges generated by ionizing radiation", *IEEE Tran. Nucl. Sci.*, vol. 23, pp. 1563-1567, 1976.
[34] D. L. Griscom, "Optical properties and structure of defects in silica glass", *J. Ceram. Soc. Japan*, vol. 99, pp. 923-941, 1991.
[35] R. Helms and E.H. Poindexter, "The silicon-silicon-dioxide system: its microstructure and imperfections", *Rep. Prog. Phys.*, vol. 57, pp. 791-852, 1994.
[36] R. A. Weeks, "Paramagnetic resonance of lattice defects in irradiated quartz", *J. Appl. Phys.*, vol. 27, pp. 1376-1381, 1959.
[37] H. E. Boesch, Jr, F.B. McLean, J.M. McGarrity and G.A. Ausman, Jr,"Hole transport and charge relaxation in irradiated SiO_2 MOS capacitors", *IEEE Trans. Nucl. Sci.*, vol. 22, pp. 2163-2167, 1975.
[38] W. L. Warren and P.M. Lenahan, "A comparison of positive charge generation in high field stressing and ionizing radiation on MOS structure", *IEEE Trans. Nucl. Sci.*, vol. 34, pp. 1355-1358, 1987.
[39] L. P. Trombetta, F.J. Feigl and R.J. Zeto, "Positive charge generation in metal-oxide-semiconductor capacitors, *J. Appl. Phys.*, vol. 69, pp. 2512-2521, 1991.
[40] R. K. Freitag, D.B. Brown and C.M. Dosier, "Experimental evidence of two species of radiation induced trapped positive charge", *IEEE Trans. Nucl. Sci.*, vol. 40, pp. 1316-1322, 1993.
[41] R. K. Freitag, D.B. Brown and C.M. Doser, "Evidence for two types of radiation-induced trapped positive charge", *IEEE Trans. Nucl. Sci.*, vol. 41, pp. 1828-1834, 1994.
[42] J. E. Conley, P.M. Lenahan, A.H. Lelis and T.R. Oldham, "Electron spin resonance evidence for the structure of a switching oxide trap: long term structural charge at silicon dangling bond sites in SiO_2", *Appl. Phys. Lett.*, vol. 67, pp. 2179-2181, 1995.
[43] J. F. Conley, P.M. Lenahan, A.J. Lelis and T.R. Oldham, "Electron spin resonance evidence that E_γ' center can behave as switching oxide trap", *IEEE Trans. Nucl. Sci.*, vol. 42, pp. 1744-1749, 1995.
[44] D. A. Buchanan, A.D. Marwick, D.J. DiMaria and L. Dori, "Hot-electron-induced hydrogen redistribution and defect generation in metal-oxide-semiconductors", *J. Appl. Phys.*, vol. 76, pp. 3595-3605, 1994.
[45] D. J. DiMaria, D.A. Buchanan, J.H. Stathis and R.E. Stahlbush, "Interface states induced by the presence of trapped holes near the silicon-silicon-dioxide interface", *J. Appl. Phys.*, vol. 77, pp. 2032-2040, 1995.
[46] S.K. Lai, "Two carrier nature of interface-state generation in hole trapping and radiation damage", *Appl. Phys. Lett.*, vol. 39, pp. 58-60, 1981.
[47] S. K. Lai, Interface trap generation in silicon dioxide when electrons are captured by trapped holes", *J. Appl. Phys.*, vol. 54, pp. 2540-2546, 1983.
[48] S. T. Chang, J.K. Wu and S.A. Lyon, "Amphoterical defects at Si-SiO_2", *Appl. Phys. Lett.*, vol. 52, pp. 622-624, 1986.
[49] S. J. Wang, J.M. Sung and S.A. Lyon, "Relationship between hole trapping and interface state generation in metal-oxide-silicon structures, *Appl. Phys. Lett.*, vol. 52, pp. 1431-1433, 1986.
[50] F. B. McLean, "A framework for understanding radiation-induced interface states in SiO_2 MOS structures, *IEEE Trans. Nucl. Sci.*, vol. 27, pp. 1651-1657, 1980.
[51] N. S. Saks, C.M. Dozier and D.B. Brown, "Time dependence of interface trap formation in MOSFETs following pulsed irradiation", *IEEE Trans. Nucl. Sci.*, vol. 35, no. 6, pp. 1168-1177, 1988.
[52] N. S. Saks and D.B. Brown, "Interface trap formation via the two-stage H^+ process", *IEEE Tran. Nucl. Sci.*, vol. 36, no. 6, pp. 1848-1857, 1989.

[53] D. L. Griscom, D.B. Brown and N.S. Saks, *Nature of radiation-induced point deffcts in amorphous SiO_2 and their role in SiO_2-on-Si structure,The Physics and Chemistry of SiO_2 and Si- SiO_2 interface*, ed C.R. Holmes and B.E. Deal, Ney-York, Plenum, 1988.
[54] K. L. Brower and S.M. Mayers, "Chemsical kinetics of hydrogen and (111) Si- SiO_2 interface defect", *Appl. Phys. Lett.*, vol. 57, pp. 162-164, 1990.
[55] J. H. Stathis and E. Cartier, "Atomic hydrogen reactions with P_b centers at the (100) Si- SiO_2 interface", *Phys. Rev. Lett.*, vol. 72, pp. 2745-2748, 1994.
[56] E. H. Poindexter, "Chemical reactions of hydrogenous species in the Si- SiO_2 system", *J. Non. Cryst. Solids*, vol. 187, pp. 257-263, 1995.
[57] R. E. Stahlbush, A.H. Edwards, D.L. Griscom and B.J. Mrstik, "Post-irradiation cracking of H_2 and formation of interface states in irradiated metal-oxide-semiconductor field-effect transistors", *J. Appl. Phys.*, vol. 73, pp. 658-667, 1993.
[58] M. M. Pejović, "Physico-chemical processes in vertical-double-diffusion metal-oxide-semiconductor field effect transistors induced by gamma-ray irradiation and post-irradiation annealing", *Facta Universitatis, Series: Physics, Chemistry and Technology*, vol. 13, pp. 13-27, 2015.
[59] McWhorter and P.S. Winocur, "Simple technique for separating the effects of interface traps and trapped-oxide charge in metal-oxide semiconductor transistors", *Appl. Phys. Lett.*, vol. 48, pp. 133-135, 1986.
[60] M. V. Fischetti, R. Gastaldi, F. Maggoni and A. Madelli, "Slow and fasdt states induced by hot electrons at Si- SiO_2 inteface", *J. Appl. Phys.*, vol. 53, pp. 3136-3144, 1982.
[61] L. P. Trombetta, F.J. Feigl and R.J. Zeto, "Positive charge generation in metal-oxide-semiconductor capacitors", *J. Appl. Phys.*, vol. 69, pp. 2512-2521, 1991.
[62] R. K. Freitag, D.B. Brown and C.M. Dozier, "Experimental evidence of two species of radiation induced trapped positive charge", *IEEE Tran. Nucl. Sci.*, vol. 40, pp. 1316-1322, 1993.
[63] A.J. Lelis. and T.R. Oldham, "Time dependence of switching oxide traps", *IEEE Tran. Nucl. Sci.*, vol. 41, pp. 1835-1843, 1994.
[64] D. M. Fleetwood, "Border traps in MOS devices", *IEEE Tran. Nucl. Sci.*, vol. 39, 269-271, 1992.
[65] V. Davidovic, Ph. D., University of Nis, 2010.
[66] S. M. Sze, *Physics of Semiconductor Devices*, Ney York, Wiley, 1981.
[67] A. Holmes-Siedle and L. Adams, *Handbook of Radiation Effects*, 2nd ed., New York: Oxford University Press, 2002.
[68] M.A.B. Eliot, "The use charge pumping currents to measure surface state densities in MOS transistors", *Solid-State Electron.*, vol. 19, pp. 241-247, 1986.
[69] J.S. Brugler and P.G. Jespres, "Charge pumping in MOS devices", *IEEE Trans. Electron DEv. Lett.*, vol. 13, pp. 627-629, 1969.
[70] G. Groeseneken, H.E. Maes, N. Baltron and R.F. De Keersmaeeker, "A reliable approch to charge-pumping measurements in MOS transistors", *IEEE Trans. Electron Dev.*, vol. 31, pp. 42-53, 1984.
[71] R. E. Paulsen, R.R. Siergiej, M.L. French andM.H. White, "Observation of near-interface oxide traps with the change pumping technique", *IEEE Electron Dev. Lett.*, vol. 13, pp. 627-629, 1992.
[72] D. Habaš, Z. Prijić, D. Pantić and N. Stojadinović, "Charge-pumping characterization of SiO_2/Si interface virgin and irradiated power VDMOSFETs", *IEEE Trans. Electron Dev.*, vol. 43, pp. 2197-2208, 1996.
[73] S. C. Witezak, K.F. Gallawoy, R.D. Schrimpf and J.R. Brews, G. Prevost, " The determination of Si-SiO_2 interface trap density in irradiated four-terminal VDMOSFETs using charge pumping", *IEEE Trans. Nucl. Sci.*, vol. 43, pp. 2558-2564, 1996.
[74] G. S. Ristić, M.M. Pejović and A.B. Jakšić, „Comparison between post-irradiation annealing and post-high electrical field stress annealing of n-channel power VDMOSFETs", *Appl. Surf. Sci.*, vol. 220, pp. 181-185, 2003.
[75] A. Kelleher, M. O'Sullivan, J. Rayn, B. O'Neal and W. Lane, "Development of the radiation sensitivity of pMOS dosimeters", *IEEE Tran. Nucl. Sci.*, vol. 39, pp. 342-346, 1992.
[76] I. Thomson, "Direct reading dosimeters", European Patent Office, Ep0471957A2, 02/07/1991.
[77] S. Best, A. Ralson and N. Suchowerska, "Clinical application of the one dose patient dosimetry system for total body irradistion", *Phys. in Medic. and Biology*, vol. 50, pp. 5909-5919, 2005.
[78] M. M. Pejović, "The gamma-ray irradiation sensitivity and dosimetric information instability of RADFET dosimeter", *Nucl. Technol. and Radiat. Protection*, vol. 28, pp. 415-421, 2013.
[79] I. Thomson, R.E. Thomson and L. P. Brendt, "Radiation dosimetry with MOS sensors", *Radiation Protec. Dosimetry*, vol. 6, pp. 121-124, 1983.
[80] L. S. August, R.R. Circle and J.C. Ritter, "An MOS dosimeter for use in space", *IEEE Tran. Nucl. Sci.*, vol. 30, pp. 508-511, 1983.

[81] L. S. August, "Estimating and reducing errors in MOS dosimeters caused by exposure to different radiations", *IEEE Trans. Nucl. Sci.*, vol. 29, no. 6, pp. 2000-2003, 1982.
[82] G. Sarrabayrouse, A. Bellaouar and P. Rossel, "Electrical properties of MOS radiation dosimeters", *Revue Phys. Appl.*, vol. 21, pp. 283-287, 1986.
[83] A. Ballaouar, G. Sarrabayrouse and P. Rassel, "MOS transistor for ionizing radiation dosimetry", Proc. 13th Yugoslav Conf. on Mictoelectronics (MIEL 85), Ljubljana, pp. 161-168, 1985.
[84] L. Adams and A. Holmes-Siedle, "The development of MOS dosimetry unit for use in space", *IEEE Trans. Nucl. Sci.*, vol. 18, pp. 1607-1612, 1978.
[85] L. Adams, E.J. Daly, R. Harboe-Sorensen, A.G. Holmes-Siedle, A.K. Ward and A.A. Bull, "Measurements of SEU and total dose in geostationary orbit under normal and solar frame conditions", *IEEE Trans. Nucl. Sci.*, vol. 38, pp. 1686-1692, 1991.
[86] J. S. Leffler, S.R. Lendgren and A.G. Holmes-Siedle, "The aplications of RADFET dosimetry to equipment radiation qualification and monitoring", *Trans. of the American Society*, vol. 60, pp. 535-536, 1989.
[87] A. G. Holmes-Siedle, L. Adams, J.S. Leffler and S.R. Lingren, "The RADFET system for real-time dosimetry in nuclear facilities", 7th Annual ASTM-Euratom Symp. on Reac. Dosimetry, Strasbourg, pp. 851-859, 1990.
[88] G. Ristić, S. Golubović and M. Pejović, "P-channel metal-oxide-semiconductor detector fading dependencies on gate bias and oxide thickness", *Appl. Phys. Lett.*, vol. 66, pp. 88-89, 1995.
[89] G. Ristić, S. Golubović and M. Pejović, "Sensitivity and fading of pMOS dosimeters with thick gate oxide", *Sensors and Actuators A*, vol. 51, pp. 153-158, 1996.
[90] Z. Savić, S. Stanković, M. Kovačević and M. Petrović, „Energy dependence of pMOS dosimeters", *Radiation Protect. Dosimetry*, vol. 64, pp. 205-211, 1996.
[91] M. M. Pejović and M. M. Pejović, „Radiation-sensitive field effect transistor response to gamma-ray irradiation", *Nuclear Technol. and Radiat. Protection*, vol. 26, pp. 25-31, 2011.
[92] M. M. Pejović, „Dose response, radiation sensitivity and signal fading of p-channal MOSFETs (RADFRTs) irradiated up to 50 Gy with ^{60}Co", *Appl. Radiation and Isotopes*, vol. 104, 100-115, 2015.
[93] S. Pejović, P. Bošnjaković, O. Ciraj-Bjelac and M.M. Pejović, "Characteristics of a pMOSFET suitable for use in radiotherapy", *Appl. Radiation and Isotopes*, vol. 77, pp. 44-49, 2013.
[94] G. Ristić, A. Jakšić and M. Pejović, „pMOS dosimetric transistors with two-layer gate oxide", *Sensors and Actuators A*, vol. 63, pp. 129-134, 1997.
[95] M. M. Pejović, S.M. Pejović, D. Stojanov and O. Ciraj-Bjelac, "Sensitivity of RADFETs for gamma and X-ray doses used in medicine", *Nuclear Technol. and Radiat. Protection*, vol. 29, pp. 179-185, 2014.
[96] M. Pejović, O. Ciraj-Bjelac, M. Kovačević, Z. Rajović and G. Ilić, "Sensitivity of P-channel MOSFET to X- and gamma-ray irradiation", *International Journal of Photoenergy*, vol. 2013, pp. 1-6, 2013.
[97] C. Ehringfeld, S. Schmid, K. Poljanc, Ch. Kirisits, H. Aiginger and D. Georg, "Application of commercial MOSFET detectors in vivo dosimetry in the therapic X-ray range from 80 kV to 250 kV, *Physics in Medicine and Biology*, vol. 50, pp. 289-303, 2005.
[98] S. M. Pejović, M.M. Pejović, D. Stojanov and O. Ciraj-Bjelac, "Sensitivity and fading of PMOS dosimeters irradiated with X-ray radiation doses from 1 to 100 cGy", *Radiation Protect. Dosimetry*, vol. 168, pp. 33-39, 2016.
[99] P. J. McWhorter, S.L. Miller and W.M. Miller, "Modeling the anneal of radiation-induced traps holes in a varying thermal environment", *IEEE Trans. Nucl. Sci.*, vol. 37, pp. 16821689, 1990.
[100] M. M. Pejović, M. M. Pejović and A.B. Jakšić, "Response of pMOS dosimeters on gamma-ray irradiation during its re-use", *Radiation Protection Dosimetry*, vol. 155, pp. 394-403, 2013.
[101] J. Aristu, F. Calvo, R. Martinez, J. Dubois, M. Santors, S. Fisher, et al., "Lung cancer, in; *Intraoperative Irradiation Techniques and Results*, 437-453, 1999.
[102] L. J. Asensio, M.A. Carvajal, J.A. Lopez-Villaneva, M. Vilches, A.M. Lallena and A.J. Palma, „Evaluation of a low-cost commercial mosfet as radiation dosimeter", *Sensors and Actuators A*, vol. 125, pp. 288-295, 2006.
[103] M. S. Martinez-Garcia, F. Simancos, A.J. palma, A.M. Lallena, J. Banqueri and M.A. Carvajal, „ General purpose MOSFETs for the dosimetry of electron beams used in intra-operative radiotherapy", *Sensors and Actuators A*, vol. 210, pp. 175-181, 2014.
[104] M. M. Pejović, „Application of p-channel power VDMOSFET as a high radiation dose sensor", *IEEE Trans. Nucl. Sci.*, vol. 62, pp. 1905-1910, 2015.